

# Blind Dockings of Benzothiazoles to Multiple Receptor Conformations of Triosephosphate Isomerase from *Trypanosoma cruzi* and Human

Zeynep Kurkcuoglu,<sup>[a, d]</sup> Gulgun Ural,<sup>[b, d]</sup> E. Demet Akten,<sup>\*[c]</sup> and Pemra Doruker<sup>\*[a, b]</sup>

**Abstract:** We aim to uncover the binding modes of benzothiazoles, which have been reported as specific inhibitors of triosephosphate isomerase from the parasite *Trypanosoma cruzi* (TcTIM), by performing blind dockings on both TcTIM and human TIM (hTIM). Detailed analysis of binding sites and specific interactions are carried out based on ensemble dockings to multiple receptor conformers obtained from molecular dynamics simulations. In TcTIM dimer dockings, the inhibitors preferentially bind to the tunnel-shaped cavity formed at the interface of the subunits, whereas non-inhibitors mostly choose other sites. In contrast, TcTIM

monomer binding interface and hTIM dimer interface do not present a specific binding site for the inhibitors. These findings point to the importance of the tunnel and of the dimeric form for inhibition of TcTIM. Specific interactions of the inhibitors and their sulfonate-free derivatives with the receptor residues indicate the significance of sulfonate group for binding affinity and positioning on the TcTIM dimer interface. One of the inhibitors also binds to the active site, which may explain its relatively higher inhibition effect on hTIM.

**Keywords:** Blind docking · Triosephosphate isomerase · *Trypanosoma cruzi* · Molecular dynamics · Benzothiazole

## 1 Introduction

Chagas Disease is a “potentially life-threatening” illness caused by the parasite *Trypanosoma cruzi* that affects about 10 million people worldwide, according to the World Health Organization reports. In the last decade, drug discovery studies have focused on parasite-specific inhibition of triosephosphate isomerase (TIM), which is a crucial enzyme in the glycolytic pathway of nearly all organisms that perform glycolysis. TIM catalyzes the interconversion of dihydroxyacetone 3-phosphate and D-glyceraldehyde 3-phosphate. TIM is a dimer formed by two identical subunits or monomers, which are made up of eight central  $\beta$ -strands that are surrounded by eight  $\alpha$ -helices. TIM is fully active in dimeric form, despite the fact that each monomer has its own catalytic site.<sup>[1]</sup> Inasmuch as, TIM exists in both human and the parasite, it becomes crucial to inhibit only *Trypanosoma cruzi* TIM's (TcTIM) activity without affecting human TIM (hTIM). Previously, it has been shown that the activity and the stability of the dimer depend on the integrity of the interface between monomers,<sup>[2]</sup> for which the interdigitating loop 3 (Gln66-Val79) plays a crucial role<sup>[2b, 3]</sup> (see Supporting Information, Figure S1a).

In general, the residues that form the interface region of oligomeric enzymes are less conserved than the residues in the active sites among the species.<sup>[2b, 4]</sup> Therefore, the interface becomes an important target region for designing new drug molecules that would specifically bind an oligomeric enzyme of a given species.<sup>[2b]</sup> Recent drug design studies have aimed at the TcTIM dimer interface that has a

specific amino acid sequence and conformation, instead of the conserved active site of the enzyme.<sup>[3–5]</sup>

In previous experimental studies, some benzothiazoles have been reported as drug candidates for the inactivation of TcTIM.<sup>[3a, 4b]</sup> Most potent inhibitors affect TcTIM activity, but not hTIM except at high concentrations,<sup>[3a]</sup> which has been related to the structural differences between TcTIM and hTIM. Specifically, at the interface where TcTIM has a cysteine residue (Cys15), hTIM has a methionine (Met15) at the same position, both of which lie near the residues of loop 3 of the other monomer. Contradictory results have

[a] Z. Kurkcuoglu, P. Doruker  
Department of Chemical Engineering and Polymer Research  
Center, Bogazici University  
Bebek, 34342, Istanbul, Turkey  
\*e-mail: doruker@boun.edu.tr

[b] G. Ural, P. Doruker  
Program of Computational Science and Engineering and Polymer  
Research Center, Bogazici University  
Bebek, 34342, Istanbul, Turkey

[c] E. Demet Akten  
Department of Information Technologies, Kadir Has University  
Cibali, 34083, Istanbul, Turkey  
\*e-mail: demet.akten@khas.edu.tr

[d] Z. Kurkcuoglu, G. Ural  
Both authors contributed equally to this work.

Supporting Information for this article is available on the WWW  
under <http://dx.doi.org/10.1002/minf.201100109>

been reported in two different mutation studies, which have aimed to reveal the effect of Cys15 on enzymatic activity.<sup>[3]</sup> Another critical structural difference between TcTIM and hTIM is the packing of the interface residues. In hTIM, the interface is more tightly packed compared to TcTIM, i.e. less accessible.<sup>[4b, 5a, b]</sup> A hydrophobic pocket (an aromatic cluster) that is crucial in the formation of a stable interface consists of Phe75 from one subunit and Tyr102 and Tyr103 of the other subunit in TcTIM. A similar pocket in hTIM comprises of Tyr67 and Phe74 from the same subunit and Phe102. The accessibility of interface in TcTIM has marked this region as a target site for drug design studies.<sup>[3–5]</sup>

In earlier computational studies, seven benzothiazoles<sup>[3a]</sup> were docked to TcTIM<sup>[5a, d]</sup> and hTIM<sup>[5a]</sup> interface, in order to reveal the differences in the binding modes and affinities. The flexible-ligand dockings were performed on a single rigid receptor conformation obtained from energy minimization.<sup>[5a]</sup> These dockings, which targeted a constricted region on the interface, emphasized that differences in the packing of aromatic clusters in TcTIM and hTIM affect the binding of inhibitors. In these docking studies, protein flexibility has not been considered,<sup>[5a, b, d]</sup> which actually needs to be taken into account for more accurate and realistic interpretations of the binding modes.

In this study, we used multiple receptor conformations from extended molecular dynamics (MD) simulations to account for both the main-chain and side-chain flexibility of the receptor in docking experiments. We performed multiple blind dockings, where the protein was held fixed and ligands were allowed to be flexible. Instead of targeting a specific region, i.e. the aromatic clusters at the interface as in previous studies,<sup>[5a, b, d]</sup> blind docking methodology was applied to determine the selectivity of benzothiazoles for the interface and other binding sites of TcTIM and hTIM. AutoDock v4.0<sup>[6]</sup> is used as the docking software in our blind dockings. The choice of AutoDock relies mainly on many records of its high performance.<sup>[7]</sup>

Furthermore, experimental studies have shown that the detrimental effect of benzothiazoles takes place during the dissociation and association of two subunits, rather than the transformation from inactive to active dimer.<sup>[3a]</sup> In order to understand the nature of the inhibition process and whether the inhibitors bind more preferentially to dimer interface or to the monomer interface that becomes accessible upon dissociation, dockings to equilibrated conformations of monomeric TcTIM were also performed. In both cases, the inhibitor will prevent the formation of a stable interface, thus the formation of a stable dimer.

Detailed analysis of TcTIM and hTIM docked poses (within 1 kcal/mol of the lowest energy conformer) was performed to reveal the differences in the binding modes of inhibitors on hTIM and TcTIM. Moreover, the role of the sulfonate group in inhibitory benzothiazoles, which has been related to increase the solubility of the benzothiazoles,<sup>[5d]</sup> was investigated in terms of the inhibition process. For this aim, dockings of sulfonate-free ligand derivatives

and a sulfonate-added derivative of non-inhibitor were performed on a TcTIM dimer conformer.

## 2 Materials and Methods

Benzothiazoles, previously reported as potential inhibitors of TcTIM,<sup>[3a, 4a]</sup> were used in this docking study and listed in Table 1. The three-dimensional structures (3D) of the ligands were obtained using the CORINA web server.<sup>[8]</sup> Among the five benzothiazoles used in this study, compounds **8**, **9** and **10** were reported as strong inhibitors of TcTIM,<sup>[3a]</sup> whereas compounds **2** and **3** were chosen as control cases without any inhibitory effect.

### 2.1 MD Simulations for Conformer Generation

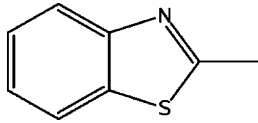
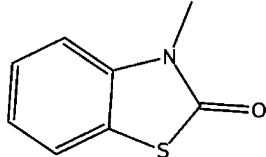
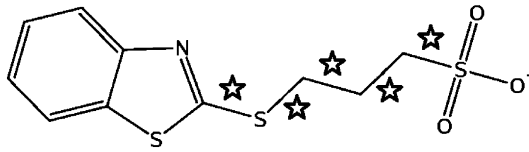
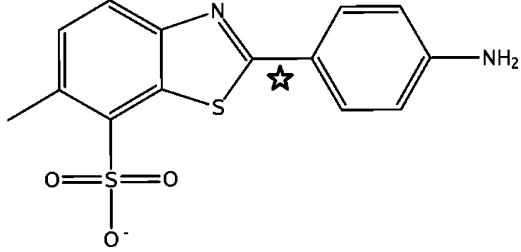
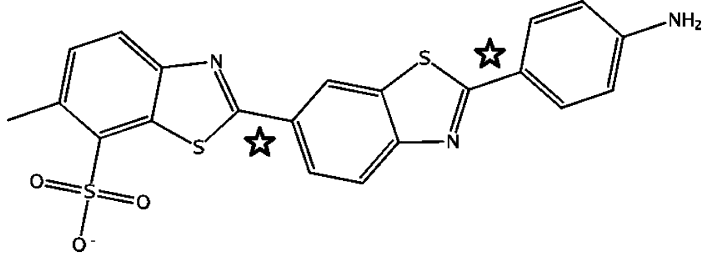
MD simulations were carried out in order to obtain distinct well-equilibrated conformers of TcTIM (monomer and dimer) and hTIM (dimer) for our docking studies. The crystal structure of apo TcTIM dimer at 1.83 Å resolution and holo hTIM dimer at 2.80 Å resolution were extracted from the Protein Data Bank (with respective PDB codes: 1TCD<sup>[9]</sup> and 1HTI<sup>[10]</sup>) and used as initial structures.

*TcTIM monomer run.* Chain A of TcTIM extracted from the dimer's crystal structure was equilibrated via 10000 steps of energy minimization and 20 ns of MD simulation using NAMD v2.6 simulation package.<sup>[11]</sup> Distinct target structures were selected from the production phase of the trajectory for docking. MD simulation was performed at constant NPT at 310 K using Langevin dynamics for all non-hydrogen atoms, with a Langevin damping coefficient of 5 ps<sup>-1</sup>. The system was kept at a constant pressure of 1 atm by using a Nose–Hoover Langevin piston<sup>[12]</sup> with a period of 100 fs and damping timescale of 50 ps. To simulate the cytoplasmic environment, the system was first solvated in a water box with dimensions of 52.4 Å × 67.7 Å × 72.1 Å and ions were added to make the overall system neutral using the plug-ins of VMD molecular visualization program.<sup>[13]</sup> CHARMM22 forcefield<sup>[14]</sup> was used to describe the interaction potential of the protein, and waters were treated explicitly using TIP3P model.<sup>[15]</sup>

Long-range electrostatic interactions were treated by the particle mesh Ewald (PME) method with a grid point density of over 1/Å. A cutoff of 12 Å was used for van der Waals and short-range electrostatics interactions with a switching function. Time step was set to 2 fs by using SHAKE algorithm for bonds involving hydrogens<sup>[16]</sup> and the data were recorded at every 1 ps. The number of time steps between each full electrostatics evaluation was set to 2. Short-range non-bonded interactions were calculated at every time step.

For monomer dockings, two snapshots were taken at 14<sup>th</sup> and 20<sup>th</sup> ns (last snapshot of the trajectory) and denoted as M1 and M2, respectively. The snapshot M1 has the highest root mean square distance ( $RMSD = 1.13$  Å) with re-

**Table 1.** Benzothiazoles used in dockings, with previously reported experimental  $IC_{50}$  values <sup>[a]</sup>.

Ligand <sup>[b]</sup>	Structure <sup>[c]</sup>	Inactivation%	$IC_{50}$ for TcTIM ( $\mu\text{M}$ )	$IC_{50}$ for hTIM ( $\mu\text{M}$ )
2		0	0	0
3		0	0	0
8		95	33	420
9		91	56	3300
10		95	8	1600

[a] The experimental  $IC_{50}$  values were taken from Tellez et al.'s study.<sup>[3a]</sup> [b] Ligand **2**: (2-methylbenzothiazole), ligand **3**: (3-methyl-2(3H)-benzothiazolone), ligand **8**: (3-(2-benzothiazolylthio)-1-propanesulfonic acid, sodium salt), ligand **9**: (2-(p-aminophenyl)-6-methylbenzothiazole-7-sulfonic acid), ligand **10**: (2-(2-(4-aminophenyl)benzothiazol-6-yl)-6-methylbenzothiazole-7-sulfonic acid, sodium salt). The same number scheme as in Tellez et al.'s study<sup>[3a]</sup> was adopted. ☆ Bonds are taken as flexible in the dockings of the present study.

spect to M2 after structural alignment based on the backbone atoms.

**TcTIM dimer run.** The dimer simulation was carried out using the AMBER<sup>[17]</sup> simulation package with the ff03 force field parameters.<sup>[18]</sup> The simulation parameters and details are the same as in a previously published simulation on chicken TIM.<sup>[19]</sup> Specifically, an NPT simulation at 300 K and 1 atm was carried out. A truncated octahedron periodic box with dimensions of 89.2 Å was used for solvation of the protein in explicit TIP3P water molecules.<sup>[15]</sup> The simulation was carried out for 13.4 ns using a time step of 2 fs.

For TcTIM dimer dockings, three snapshots were selected at 6.8<sup>th</sup>, 10.5<sup>th</sup> and 13.4<sup>th</sup> ns (denoted as D1, D2 and D3, respectively). The last snapshot (D3) exhibits RMSD values of 1.38 and 1.47 Å with respect to D1 and D2. RMSD between D1 and D2 is 1.25 Å.

**hTIM dimer run.** Same procedure as in TcTIM monomer run was applied to the crystal structure of hTIM dimer using NAMD v2.6. The periodic box dimensions were 65.8 Å × 96.6 Å × 84.1 Å. Inasmuch as a relatively longer run of 55 ns duration was performed, the selection of the conformers for hTIM was based on k-means clustering<sup>[20]</sup> of the RMSD values. First 6 ns of the MD simulation were discarded for equilibration. The clustering was performed by using the MMTSB toolset.<sup>[21]</sup> The conformations were clustered according to 2 Å RMSD, with respect to the centroid (average) structure in each cluster leading to three clusters with 988, 575 and 71 elements. One representative snapshot was taken from each cluster for blind docking. These snapshots named as H1 (at 20<sup>th</sup> ns), H2 (at 21.7<sup>th</sup> ns) and H3 (at 35.8<sup>th</sup> ns) have the lowest RMSD value with respect to the centroid structure in the corresponding clusters. The RMSD

between H1-H2, H1-H3 and H2-H3 are 1.14, 1.19 and 1.59 Å, respectively.

## 2.2 Docking

In blind dockings, the target region was selected as the whole protein for the monomer case, whereas one of the monomers and the interface region were selected for the dimer cases, as illustrated in Figure S1. Ligands were held flexible and rotatable bonds are shown in Table 1.

In all docking experiments, the Lamarckian genetic algorithm of AutoDock v4.0<sup>[6]</sup> was used to explore the conformational space. 100 runs were performed for each docking with each run consisting of  $26 \times 10^6$  energy evaluations. Grid box constructed with a spacing of 0.375 Å has dimensions of 126 Å  $\times$  126 Å  $\times$  126 Å for all monomer and dimer dockings (Figure S1).

In order to determine the residues that lie on the interface region between the subunits, SASA differences<sup>[22]</sup> between monomer and dimer forms are calculated, both in crystal structure and chosen conformers. A total of 47 residues were chosen as the interface residues, namely Asn12-Ser20, Thr45-Met51, Gln66-Ser80, Gln82-Leu84, Asp86, Tyr87, Ile89, Val93, His96, Glu98, Arg99, Tyr102-Thr106 and Lys113 for TcTIM and 42 residues for hTIM, namely Asn11, Lys13-Gln19, Pro44-Phe50, Gln53, Gln64-Ser79, Gly81-Ile83, Asp85, Cys86, Val92, His95, Glu97, Arg98, Val101, Phe102 and Lys112.

For each docking experiment, the conformations were clustered according to 2 Å RMSD with respect to the lowest energy conformation in that cluster. Only the highest ranked clusters within 1 kcal/mol of the lowest energy conformer were chosen for the binding mode analysis. The interactions between the lowest energy conformer of every cluster and the ligand were illustrated in 2D using MOE software tool,<sup>[23]</sup> using a threshold value of 4.5 Å for maximum interaction distance. To detect how often each residue interacts with the ligand, the percentage of occurrence was calculated among the conformations within 1 kcal/mol using the following equality,

$$\% \text{ occurrence} = 100 \times \text{NR}/\text{NT} \quad (1)$$

where NR is the number of conformers in which a specific residue lies within the threshold and NT is the total number of conformers within 1 kcal/mol.

The percentage of occurrence was also calculated to determine how often the ligand selects a specified region. For this purpose, percentage of occurrence was taken as the ratio of the number of conformations in which ligand selects the specified region over the total number of conformations. In hTIM case, the ratio was also weighted according to number of elements in MD clusters that the conformers were selected from.

## 3 Results and Discussion

### 3.1 TcTIM Dimer Dockings

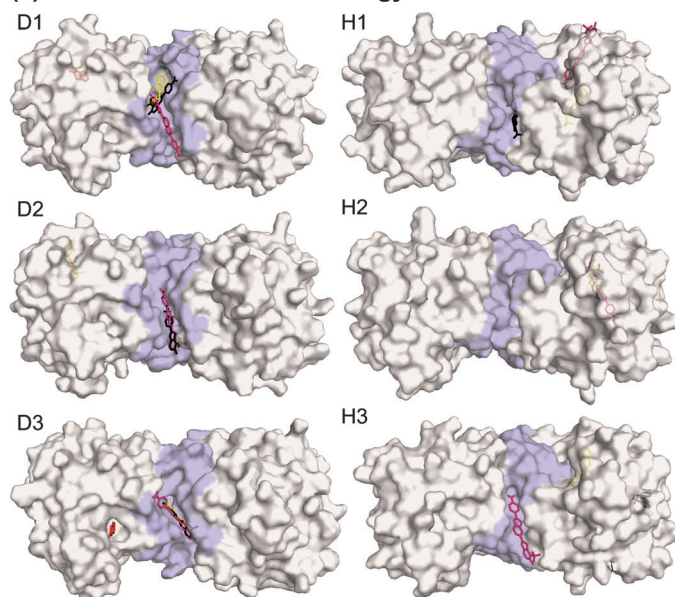
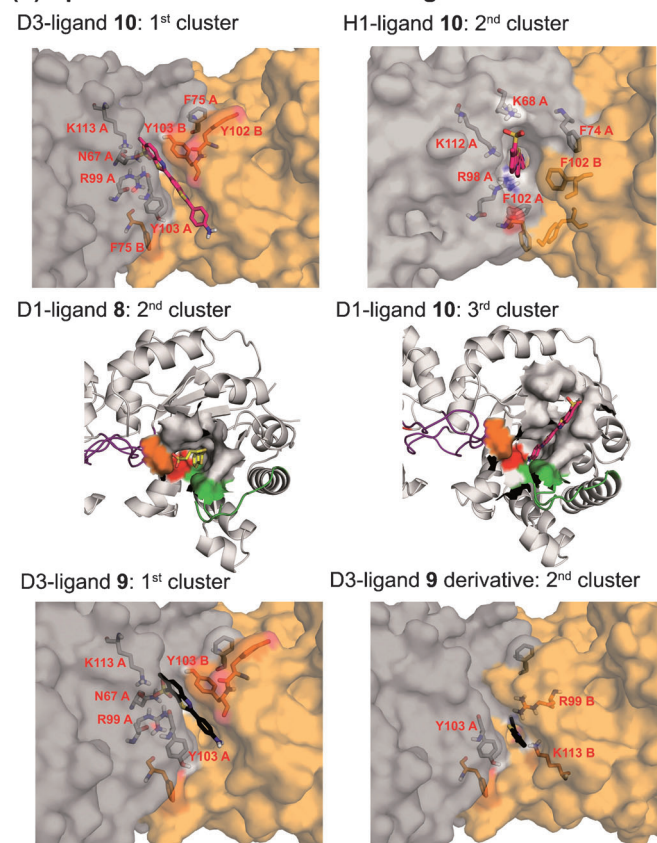
In blind dimer dockings, the grid box covers an entire monomer and the interface region between monomers in order to reveal possible binding sites for each ligand. The left panel of Figure 1a shows the location of the best pose of each ligand docked against three MD conformers D1, D2 and D3. The inhibitory ligands (except ligand **8** docked to conformer D2) tend to lie along the tunnel-shaped cavity at the interface formed by the residues of loop 3 and Arg99, Tyr102-Thr106, Lys113, whereas the non-inhibitory ligands do not choose this region.

In Table 2, several binding sites are classified for each ligand using its MOE 2D interaction diagrams (based on clusters within 1 kcal/mol). The occurrence at the tunnel-shaped cavity is reported as 48%, 74% and 89% for the inhibitors **8**, **9** and **10**, respectively. In contrast, the non-inhibitory ligands select this region with lower percentages and prefer other sites such as A and B listed in Table 2. This clearly indicates the importance of the tunnel for the inhibition process. These binding sites are shown in Figure 2a, where the occurrence percentage of each residue (Equation 1) is shown using a color-coded surface representation of the enzyme. Among the inhibitors, ligand **8** selects a broader region of the tunnel, possibly due to its flexibility. In a crystal structure of TcTIM, ligand **8** is reported to bind to the external portion of the tunnel<sup>[4a]</sup> (see Figure S1b), which is also observed by our docking results. Moreover, the x-ray structure of TcTIM crystallized in hexane revealed two hexane molecules near residues Ile69, Phe75, Tyr103, Gly104, Lys113 of one monomer and Tyr102, Tyr103 of the other monomer<sup>[24]</sup> (see Figure S1b). These residues correspond to the warm-colored region of the tunnel, especially for ligand **9** and ligand **10** in Figure 2a.

The catalytic region presents a cavity that is preferred by ligands **8** and **10** with an occurrence percentage of 19 and 11, respectively. Binding poses on this catalytic site of D1 are shown in Figure 1b. Due to its flexibility, ligand **8** fits into this cavity, thereby possibly inhibits the entry of the substrate to the active site and the closure of loop 6 over the catalytic site. In contrast, the binding mode of ligand **10** on the catalytic region seems more solvent-exposed. We performed a preliminary 10-ns simulation on this D1-ligand **10** complex, which has revealed an instable complex with movement of ligand **10** to other regions.

The difference in the binding modes among inhibitors is that ligand **10** concentrates mainly on the tunnel, whereas ligands **8** and **9** also select different sites. This fact may be reflected on the reported  $IC_{50}$  values,<sup>[3a]</sup> also given in Table 1. Relatively lower  $IC_{50}$  value for ligand **10** may be related with its selective behavior for the interface region.

Previous studies, in which the dockings have been specifically targeted to the tunnel region of the interface, have reported that the ligands **8**, **9** and **10** make  $\pi$ - $\pi$  interac-

**(a) TcTIM and hTIM lowest energy conformations****(b) Specific interactions and binding modes****Table 2.** Binding sites of inhibitory ligands on TcTIM dimer (occurrence percentages).

Ligand	Tunnel shaped cavity on the interface <sup>[a]</sup>	Catalytic site <sup>[b]</sup>	Region A <sup>[c]</sup>	Region B <sup>[d]</sup>	Other
2	12	0	11	30	47
3	22	3	40	25	10
8	48	19	26	7	0
9	74	5	14	7	0
10	89	11	0	0	0

[a] Loop 3, Arg99, Tyr102–Thr106 and Lys113; [b] Lys14, His96 and Glu168; [c] Lys53, Leu56–Asn58, Phe61–Ile63 and Tyr87–Ser90; [d] Lys157–Val163 and Arg208.

tions with Tyr103 and “possible” cation– $\pi$  interactions with Arg99, Lys113 and that the sulfonate group of these ligands interacts with Arg71 and Phe75.<sup>[5a]</sup> We performed a detailed analysis of specific interactions (H-bonding,  $\pi$ – $\pi$  and cation– $\pi$  interactions, according to criteria described elsewhere<sup>[5e, f, 7a]</sup>) between ligand and receptor (Tables S2–S4) using all conformers that fall within 1 kcal/mol of the lowest energy one. As reported in Table S2, all ligands except **2** are able to make H-bonding with the receptor residues. The non-inhibitory ligand **3** mostly makes H-bonds with Lys14, Met51, Thr70 and Arg71. Sulfonate group of ligands **8**, **9** and **10** makes multiple H-bonding with Asn67, Thr70 (except ligand **8**), Arg71 (only for ligand **8**), Arg99 and Lys113. Considering the number of H-bonds per conformation, ligand **3** has the lowest ratio (0.17), whereas the inhibitors exhibit a ratio around 1.00. In addition, the MOE 2D diagrams (Figure S2) for lowest energy conformers clearly indicate the multiple H-bonding pattern for sulfonate group of the inhibitors. Thus, we suspect that the sulfonate group may contribute to the specificity and the binding affinity of the inhibitors, besides facilitating the dissolution of the ligands as stated in previous works.<sup>[5d]</sup> To investigate this issue further, blind dockings of several ligand derivatives onto the conformer D3 have been also performed as will be discussed in the following section.

**Figure 1.** (a) TcTIM and hTIM dimer dockings: Lowest energy conformations for D1, H1, D2, H2, D3 and H3. The interface region is shown in light blue together with ligand **2** (red), ligand **3** (green), ligand **8** (yellow), ligand **9** (black) and ligand **10** (warmpink). In the left panel, inhibitory ligands lie along the tunnel on the interface of TcTIM. (b) Specific interactions and binding modes for ligand **10** on conformers D3 (1<sup>st</sup> cluster) and H1 (2<sup>nd</sup> cluster) indicate that there is a change in the binding mode of inhibitory ligand **10**; it lies along the tunnel on the interface of TcTIM, whereas it binds in a perpendicular manner to the cavity on the interface of hTIM. Binding poses of ligand **8** (2<sup>nd</sup> cluster), and ligand **10** (3<sup>rd</sup> cluster) on TcTIM active site for conformer D1: Ligand **8** fits into the cavity on the catalytic site, however ligand **10** binds to the same cavity in a more solvent-exposed position. Specific interactions and binding modes of ligand **9** (1<sup>st</sup> cluster) and ligand **9** derivative (2<sup>nd</sup> cluster) on conformer D3: Lack of sulfonate group changes the binding mode of the ligand **9** from parallel to perpendicular.

Besides H-bonding, ligands are able to make  $\pi$ - $\pi$  and cation- $\pi$  interactions with the receptor residues. Inhibitory ligands (**8**, **9** and **10**) make  $\pi$ - $\pi$  interactions mostly with Phe75 and Tyr103 (Table S3). These residues that belong to the aromatic cluster at the interface (formed by Phe75 of one chain and Tyr102 and Tyr103 from the other chain) have already been stated to be important for the stability of the dimer in the previous works.<sup>[4b, 5a, b, d]</sup> From Table S4, all inhibitory ligands make cation- $\pi$  interactions with Arg99 and Lys113. Different from other ligands, ligand **8** makes cation- $\pi$  interactions with catalytic Lys14 and  $\pi$ - $\pi$  interactions with catalytic His96. It also makes cation- $\pi$  interactions with Lys53. Thus, ligand **8** shows deviations from other inhibitory ligands in terms of its preference for receptor residues to interact with. In this context, ligand **8** has a potential to bind diverse sites, instead of focusing the interface region.

The non-inhibitory ligands interact with different residues compared to inhibitors. For example, ligand **2** makes  $\pi$ - $\pi$  interactions with Phe46, His48 and Tyr87 and cation- $\pi$  interactions with Arg100, which is completely different than inhibitory ligands' behavior. Ligand **3** makes  $\pi$ - $\pi$  interactions with Tyr103 and cation- $\pi$  interactions with Arg99, but in 31% of the conformations, it also interacts with Tyr87.

Moreover, the higher number of  $\pi$ - $\pi$  interactions observed per conformation suggest that  $\pi$ - $\pi$  interactions are more dominant compared to cation- $\pi$  interactions (e.g. for ligand **10**,  $\pi$ - $\pi$  ratio is 4.54 whereas it is only 0.84 for cation- $\pi$ ; see Tables S3 and S4 for more detail).

### 3.2 TcTIM Dimer Dockings with Derivatives of Ligands

To assess the importance of the sulfonate group on the binding affinity of benzothiazoles and the selectivity for the interface region, derivatives of ligands **2**, **8**, **9** and **10** were created using CORINA web server.<sup>[6]</sup> A sulfonate group was added to ligand **2** (i.e. it became 2-methylbenzothiazole-7-sulfonic acid), whereas the sulfonate group was removed from the inhibitors. Derivatives were docked to D3 conformer using the same blind docking methodology. The residues that interact with the ligand are color-coded according to percentage occurrence values in Figure 2b. The left and right panels compare the original results of the conformer D3 with results of the derivatives docked to the same conformer, respectively.

As explained in the previous section, ligand **2** is able to bind to various regions on the dimer. However, addition of a sulfonate group to ligand **2** increases its selectivity for the interface region, as shown in Figure 2b. In accordance, the deletion of the sulfonate group from ligand **10** decreases its selectivity for the tunnel region of the interface. These results clearly indicate that the presence of sulfonate group is critical for positioning of the ligands in the tunnel via specific H-bonding besides the aromatic interactions.

For derivatives of ligands **8**, **9** and **10**, although high occurrence percentages are present for certain residues at the interface, they do not pursue the binding pattern observed for the ligands containing the sulfonate group. As shown in Figure 1a and Figure 1b, ligands **8**, **9** and **10** lie along the tunnel shaped cavity on the interface, while in the majority of the derivative conformers at the interface (82%, 59%, 55%, respectively) the binding occurs in a perpendicular manner (Figure 1b). This type of orientation causes a more localized interaction area, which is well reflected by the varying degrees of occurrences in Figure 2b. Thus, the absence of sulfonate group decreases the selectivity for the interface region and changes the binding mode of the ligands.

Moreover, the estimated free energies of binding for the best conformers of original ligands on the interface are found to be appreciably lower than those of the sulfonate-free ligands, as shown in Table 3. This clearly indicates that the sulfonate group adds more stability (binding affinity) to the protein-inhibitor complexes.

**Table 3.** Docking scores of ligands and their derivatives for TcTIM dimer (D<sub>3</sub>) dockings.

Ligand	$\Delta G^{[a]}$ for original ligands on D3	$\Delta G^{[a]}$ for derivatives on D3
2	-4.55 (3 <sup>rd</sup> cluster)	-5.74 (2 <sup>nd</sup> cluster)
8	-7.10 (1 <sup>st</sup> cluster)	-5.23 (3 <sup>rd</sup> cluster)
9	-7.67 (1 <sup>st</sup> cluster)	-6.03 (2 <sup>nd</sup> cluster)
10	-9.27 (1 <sup>st</sup> cluster)	-7.19 (1 <sup>st</sup> cluster)

[a]  $\Delta G$  is the estimated free energy of binding in AutoDock (kcal/mol), which is also used as a score. Reported  $\Delta G$  values belong to the lowest energy conformation at the interface.

### 3.3 hTIM Dimer Dockings

Blind docking methodology is applied to hTIM dimer conformers in order to investigate the binding modes of the inhibitors in comparison with the TcTIM dimer case. In Table 4, binding sites of the inhibitors on hTIM dimer are listed and these binding sites are shown in Figure 2c.

Contrary to TcTIM results, the inhibitory ligands **8**, **9** and **10** select the cavity at the interface only in 3%, 14% and 32% of the conformations, respectively. Moreover, the binding modes of the ligands are also quite different; in 63%, 81% and 60% of the conformers a perpendicular binding mode is observed. Examples of this binding mode are provided in Figure 1a for H1-ligand **9** (lowest energy conformer), and in Figure 1b for H1-ligand **10** (2<sup>nd</sup> cluster conformer). In these conformers, the sulfonate group does not make multiple H-bonding with the receptor residues as observed in the TcTIM dimer case (see Figure S3 for MOE 2D interaction diagrams)

Similar to the TcTIM dimer results, catalytic site is again a preferred binding site for ligands **8** and **10** with occurrence



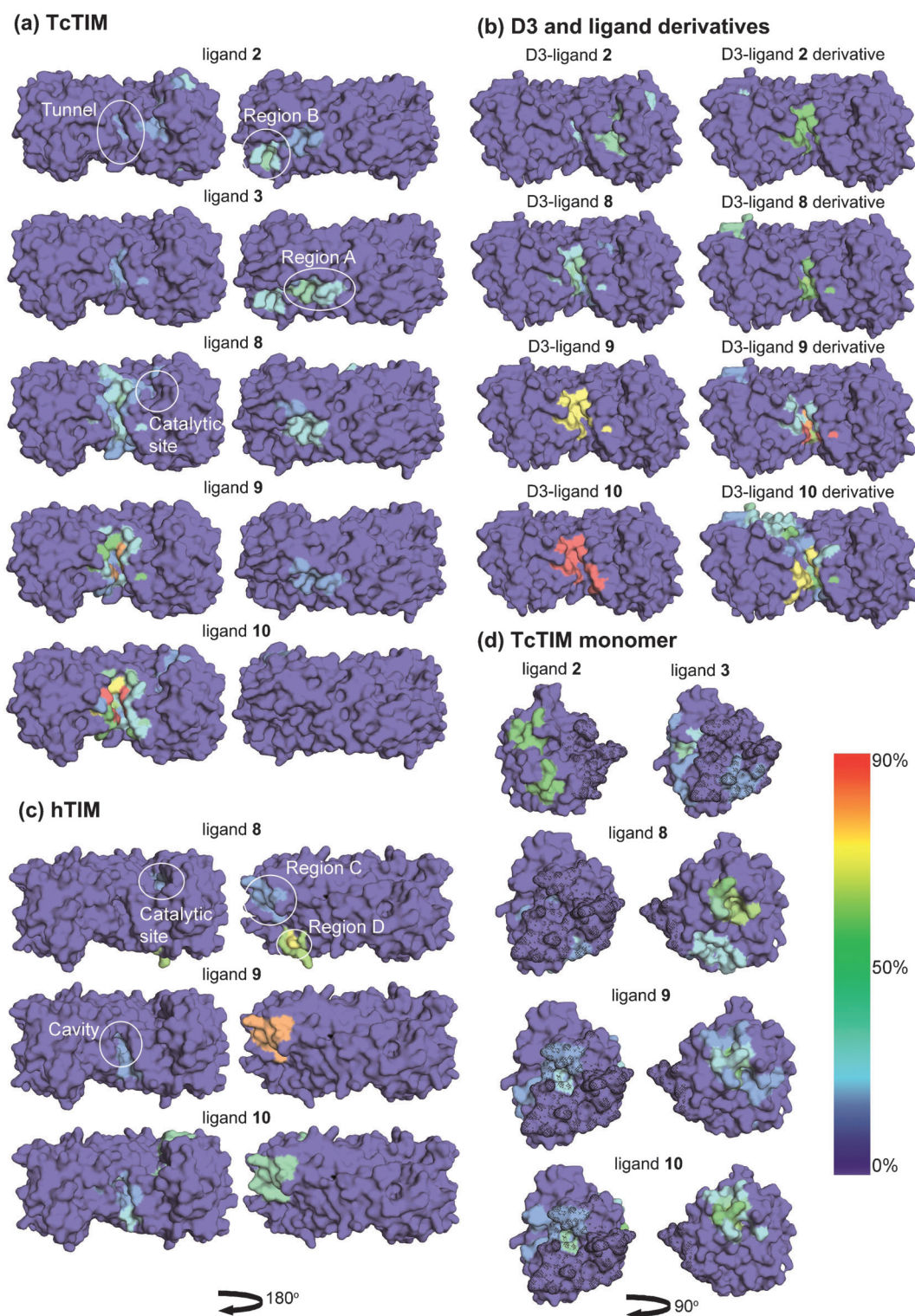


**Figure 2.** (a) Occurrence density of ligands **2**, **3**, **8**, **9** and **10** on TcTIM dimer (averaged over conformers D1, D2, D3): The left panels focus on the tunnel-region from the same viewpoint as in Figure 1 a, whereas the right panels show other binding sites on the opposite side of the protein (180° rotation). (b) Occurrence density of ligands **2**, **8**, **9** and **10** (left column) and their derivatives (right column) only on D3: Ligands with sulfonate group select a similar region along the tunnel on the interface, whereas ligands without sulfonate group either tend to bind to other regions or they bind to a narrower region on the interface. (c) Occurrence density of ligands **8**, **9** and **10** for hTIM dimer conformers (averaged over conformers H1, H2, H3): Inhibitory ligands do not generally bind to the cavity on the interface of hTIM, they prefer other sites. Ligands **8** and **10** also select the catalytic site for binding (same viewpoint as in (a)). (d) Occurrence density of ligands **2**, **3**, **8**, **9** and **10** on TcTIM monomer(averaged over conformers M1, M2): The 'interface' residues that become solvent exposed upon dissociation of the dimer are marked as black meshed surface.

**Table 4.** Binding sites of inhibitory ligands on hTIM dimer (occurrence percentages).

Ligand	Cavity on the interface <sup>[a]</sup>	Catalytic site <sup>[b]</sup>	Region C <sup>[c]</sup>	Region D <sup>[d]</sup>	Other
8	3	20	21	56	0
9	14	3	74	8	1
10	32	31	32	1	4

[a] Loop 3, Arg98, Val101, Phe102 and Lys112; [b] Lys13, His95 and Glu165; [c] Ala31-Val39 and Ile244-Gln248; [d] Asn153-Lys159 and Ser203-Arg205.

percentages of 20 and 31, respectively. The binding modes of these ligands at this site also resemble the ones in the TcTIM dimer case (Figure 1b). Flexible ligand **8** fits into the cavity on the active site, thereby seems protected against the solvent effects, whereas the binding mode of ligand **10** is more solvent-exposed. Considering the conservation of the active site residues in both TcTIM and hTIM, binding of ligand **10** to the active site of hTIM will be also instable since TcTIM-ligand **10** active site complex is not stable, as mentioned in TcTIM dimer results. In addition, the reported  $IC_{50}$  values<sup>[3a]</sup> for hTIM case, are 422  $\mu$ M, 3.3 mM, 1.6 mM for ligands **8**, **9** and **10**, respectively (Table 1), thus the ligand **8** is more effective in the inhibition of hTIM than the other inhibitors. Considering the blind docking results for the catalytic site, we suspect that ligand **8**'s effect on both hTIM and TcTIM is also related with its preference for catalytic site and its fitting binding mode on this site.

We cannot attribute a clear allosteric effect of other binding regions C and D in the inhibition process, which can be questioned by further simulations. However, based on the highest  $IC_{50}$  value of ligand **9** that mostly selects region C (by 74%), we suggest that this region is not involved in the inhibition of hTIM.

### 3.4 TcTIM Monomer Dockings

Monomeric TIM is known to be stable but not catalytically active.<sup>[25]</sup> So, monomer dockings have been performed to see whether the benzothiazoles (mainly for inhibitors **8–10**) mainly select the interface region as in the dimer case, or there exists other favorable binding sites.

As indicated above, we consider all clusters with energy values that lie within 1 kcal/mol of the lowest energy conformation for each snapshot chosen from the MD run (M1 and M2). The percentage of occurrence of each residue (averaged over clusters from M1 and M2) within 4.5 Å of the ligand is color coded on the monomer structure in Figure 2d. Non-inhibitory ligands (ligands **2** and **3**) do not prefer to bind to the interface region shown with black mesh, whereas the inhibitory ligands select the interface region in some of the clusters. In fact there are other binding sites for the inhibitors, shown in Figure 2d.

The lowest free energy of binding (which corresponds to the highest score value in AutoDock) and the fraction of

occurrence at the interface, are given separately for conformers M1 and M2 in Table S6. The inhibitors **8**, **9** and **10** choose the interface region more often compared to ligands **2** and **3** with no inhibitory effect (Table S6, Figure 2d). Specifically, ligand **2** does not bind to the interface region and ligand **3** selects the interface region in 12% of the conformations in the high scoring clusters (averaged over M1 and M2). In contrast, the ligands **8**, **9** and **10** select the interface in 29%, 29% and 38% of the conformations, respectively, with a relatively lower free energy of binding compared to ligand **3**. Thus, the interface that becomes solvent-exposed upon dimer dissociation has become one of the preferred binding sites for the inhibitory ligands, but not distinctively selected by the inhibitors, contrary to the dimer case.

Additionally, in Figure S4, 2D interaction diagrams are given for compound **8**, **9** and **10**, which interact with interface residues at a distance of 4.5 Å, for M1 and M2 conformers. It is clear that when the inhibitory ligands select the interface, they prefer to make H-bonds with Asn67, Arg99 and Lys113 and the catalytic residues Lys14 and His96. There are also  $\pi$ – $\pi$  interactions with His96 and cation– $\pi$  interactions with Arg99, Lys113.

### 3.5 Free Energies of Binding

For a comparison of all docking results (monomer and dimers), the lowest free energy of binding ( $\Delta G$ ) at the interface (averaged over different MD snapshots) is reported in Table 5. In all cases, the estimated values of the free energy of binding are appreciably lower for ligands **8**, **9** and **10** compared to non-inhibitory ligands. This may be associated to the increased number of H-bonds,  $\pi$ – $\pi$  and cation– $\pi$  interactions, between the inhibitors and the receptor residues.

We cannot distinguish between the binding affinity of inhibitors at the interface of TcTIM and hTIM from the estimated free energies. However, our blind dockings stress the preferences of inhibitors for different binding sites in TcTIM and hTIM. In this respect, the tunnel region of TcTIM is the main site of importance for all inhibitors and the catalytic site also stands out in the case of ligand **8**.

**Table 5.** Docking scores at the interface for TcTIM monomer, TcTIM dimer and hTIM dimer ( $\Delta G$ , kcal/mol).

Ligand	TcTIM monomer	TcTIM dimer	hTIM dimer
2	None at interface	–4.75	
3	–4.75	–4.82	
8	–6.96	–6.79	–7.15
9	–6.34	–7.22	–6.54
10	–7.39	–8.85	–8.13



## 4 Conclusions

In this work, we investigated the binding sites for five benzothiazoles and the differences in the binding modes of the inhibitory ligands among TcTIM monomer, TcTIM dimer and hTIM dimer. We used the blind docking methodology with multiple receptor conformations, which is different from previous interface aimed-single conformer dimer dockings.<sup>[5a, b, d]</sup> Comparison of TcTIM monomer and dimer results in terms of their preferences for the interface region suggests that the tunnel-shaped cavity at the interface of dimer presents a more favorable binding site for the inhibitors. Thus, it is most likely that the inhibitory ligands bind to the enzyme and are effective during the dissociation of the monomers, rather than their association.

TcTIM dimer results indicate that inhibitory ligands (**8**, **9** and **10**) prefer the interface region more often than the rest of the receptor and with higher binding affinity than non-inhibitors (**2** and **3**), which do not show any preference for tunnel shaped cavity on the interface. This result is in accordance with the available crystal structures of TcTIM with ligand **8** on its interface<sup>[4a]</sup> and of TcTIM soaked in hexane, where two hexane molecules are within 4.5 Å distance of interface residues.<sup>[24]</sup> This agreement serves as a validation of our docking poses. Still, we need to stress that docking studies per se present only models that are mainly affected by the limitations of the scoring function, such as simplified assumptions on the solvation effect, entropy and electrostatic interactions.<sup>[26]</sup> Preference of the inhibitors for the interface region may be related with the intensity of H-bonding and aromatic interactions between inhibitory ligands and the receptor. In TcTIM dimer, the inhibitory ligands make H-bonding especially with Asn67, Thr70, Arg71, Arg99 and Lys113 by means of their sulfonate group,  $\pi$ - $\pi$  interactions with Phe75 and Tyr103, and cation- $\pi$  interactions with Arg99 and Lys113. These interactions promote a favorable parallel positioning of all inhibitors along the tunnel.

Blind dockings of the sulfonate-free ligand derivatives on D3 reveal that ligands with sulfonate group select the interface more often and deletion of the sulfonate group changes the binding pattern, affinity and the binding mode of the inhibitors (from a parallel to a perpendicular positioning on the tunnel). This result clearly indicates that sulfonate group has an important role in interface selection and binding affinity, which has not been detected in previous studies.

Comparison of the docking results for the inhibitors on TcTIM and hTIM dimer indicates that hTIM dimer interface is less favorable than that of TcTIM, implying again the importance of interface region for selective inhibition. In contrast to TcTIM, ligand **10** exhibits a perpendicular orientation in most conformers of hTIM, which may lead to an unstable complex. This issue can be further explored via MD simulations to show that a parallel pose along the tunnel-shaped cavity is necessary for inhibition to occur. In fact,

our preliminary results based on a 100 ns MD simulation for TcTIM conformer (to be published) indicate that a complex with ligand **10** that lies along the tunnel (lowest energy conformer from our docking experiments) is stable.

Ligands **8** and **10** also choose the catalytic site in both TcTIM and hTIM, where ligand **10** is more solvent-exposed than ligand **8**. Our preliminary MD simulation results on TcTIM conformer with ligand **10** on the catalytic site indicate the instability of this complex. In contrast, ligand **8** fits deep into the cavity on the catalytic site due to its flexible nature and this may provide an additional means of inhibition. This may explain its relatively higher inhibitory effect on hTIM (see Table 1 for  $IC_{50}$  values).

## Acknowledgements

This work is partially supported by TUBITAK Project No: 109M213, DPT Project No: 2009k120520, BAP Project No: 5714 and the *Betil* fund. Grid box representations for TcTIM are prepared using ADT software<sup>[7b]</sup> and all other molecular graphics are prepared using PyMOL.<sup>[26]</sup>

## References

- [1] a) K. D. Schnackerz, R. W. Gracy, *Eur. J. Biochem.* **1991**, *199*, 231–238; b) V. Zomosa-Signoret, G. Hernandez-Alcantara, H. Reyes-Vivas, E. Martinez-Martinez, G. Garza-Ramos, R. Perez-Montfort, M. T. Gomez-Poyou, A. Gomez-Poyou, *Biochemistry* **2003**, *42*, 3311–3318.
- [2] a) V. Mainfroid, P. Terpstra, M. Beauregard, J. M. Frere, S. C. Mandé, W. G. J. Hol, J. A. Martial, K. Goraj, *J. Mol. Biol.* **1996**, *257*, 441–456; b) R. Perez-Montfort, M. T. Gomez-Puyou, A. Gomez-Puyou, *Curr. Top. Med. Chem.* **2002**, *2*, 457–470.
- [3] a) A. Tellez-Valencia, S. Avila-Rios, R. Perez-Montfort, A. Rodriguez-Romero, M. T. Gomez-Puyou, F. Lopez-Calahorra, A. Gomez-Puyou, *Biochem. Biophys. Res. Commun.* **2002**, *295*, 958–963; b) V. Olivares-Illana, A. Rodriguez-Romero, I. Becker, M. Berzunza, J. Garcia, R. Perez-Montfort, N. Cabrera, F. Lopez-Calahorra, M. T. Gomez-Puyou, A. Gomez-Puyou, *PLoS Neglected Trop. Dis.* **2007**, *1*, 1–8.
- [4] a) A. Tellez-Valencia, V. Olivares-Illana, A. Hernandez-Santoyo, R. Perez-Montfort, M. Costas, A. Rodriguez-Romero, F. Lopez-Calahorra, M. T. Gomez-Puyou, A. Gomez-Puyou, *J. Mol. Biol.* **2004**, *341*, 1355–1365; b) V. Olivares-Illana, R. Perez-Montfort, F. Lopez-Calahorra, M. Costas, A. Rodriguez-Romero, M. T. Gomez-Puyou, A. Gomez-Puyou, *Biochemistry* **2006**, *45*, 2556–2560.
- [5] a) L. M. Espinoza-Fonseca, J. G. Trujillo-Ferrera, *Biochem. Biophys. Res. Commun.* **2005**, *328*, 922–928; b) L. M. Espinoza-Fonseca, J. G. Trujillo-Ferrera, *Bioorg. Med. Chem. Lett.* **2006**, *16*, 6288–6292; c) J. Gayosso-De-Lucio, M. Torres-Valencia, A. Rojo-Dominguez, H. Najera-Pena, B. Aguirre-Lopez, J. Salas-Pacheco, C. Avitia-Dominguez, A. Tellez-Valencia, *Bioorg. Med. Chem. Lett.* **2009**, *19*, 5936–5939; d) L. M. Espinoza-Fonseca, J. G. Trujillo-Ferrera, *Bioorg. Med. Chem. Lett.* **2004**, *14*, 3151–3154; e) G. Alvarez, B. Aguirre-Lopez, J. Varela, M. Cabrera, A. Merlino, G. V. Lopez, M. L. Lavaggi, W. Porcal, R. Di Maio, M. Gonzales, H. Cerecetto, N. Cabrera, R. Perez-Monfort, M. T. de Gomez-Puyou, A. Gomez-Puyou, *Eur. J. Med. Chem.* **2010**, *45*,

- 5767–5772; f) A. Romo-Mancillasa, A. Téllez-Valencia, L. Yépez-Muliac, F. Hernández-Luisa, A. Hernández-Campos, R. Castillo, *J. Mol. Graphics Modell.* **2011**, *30*, 90–99.
- [6] G. M. Morris, R. Huey, W. Lindstrom, M. F. Sanner, R. K. Belew, D. S. Goodsell, A. J. Olson, *J. Comput. Chem.* **2009**, *30*, 2785–2791.
- [7] a) C. Hetenyi, D. van der Spoel, *Protein Sci.* **2002**, *11*, 1729–1737; b) C. Hetenyi, D. van der Spoel, *FEBS Lett.* **2006**, *580*, 1447–1450; c) M. Kovacs, J. Toth, C. Hetenyi, A. Malnasi-Csizmadia, J. R. Sellers, *J. Biol. Chem.* **2004**, *279*, 35557–35563; d) Z. Bikadi, E. Hazai, F. Zsila, S. F. Lockwood, *Bioorg. Med. Chem.* **2006**, *14*, 5451–5458; e) E. Hazai, Z. Bikadi, F. Zsila, S. F. Lockwood, *Bioorg. Med. Chem.* **2006**, *14*, 6859–6867; f) B. Iorga, D. Herlem, E. Barre, C. Guillou, *J. Mol. Model.* **2006**, *12*, 366–372; g) B. K. Paul, N. Guchhait, *J. Phys. Chem. B* **2011**, *115*, 10322–10334; h) R. M. Bieganski, M. L. Yarmush, *J. Mol. Graphics Modell.* **2011**, *29*, 965–973.
- [8] J. Sadowski, J. Gasteiger, G. Klebe, *J. Chem. Inf. Comput. Sci.* **1994**, *34*, 1000–1008.
- [9] E. Maldonado, M. Soriano-Garcia, A. Moreno, N. Cabrera, G. Garza-Ramos, M. T. Gomez-Puyou, R. Gomez-Puyou, *J. Mol. Biol.* **1998**, *283*, 193–203.
- [10] S. C. Mande, V. Mainfroid, K. H. Kalk, K. Goraj, J. A. Martial, W. G. J. Hol, *Protein Sci.* **1994**, *3*, 810–821.
- [11] J. C. Phillips, R. Braun, W. Wang, J. Gumbart, E. Tajkhorshid, E. Villa, C. Chipot, R. D. Skeel, L. Kale, K. Schulten, *J. Comput. Chem.* **2005**, *26*, 1781–1802.
- [12] S. E. Feller, Y. Zhang, R. W. Pastor, B. R. Brooks, *J. Chem. Phys.* **1995**, *103*, 4613–4621.
- [13] W. Humphrey, A. Dalke, K. Schulten, *J. Mol. Graphics* **1996**, *14*, 33–38.
- [14] A. D. MacKerell Jr., D. Bashford, R. L. Bellott, R. L. Dunbrack Jr., J. D. Evanseck, M. J. Field, S. Fischer, J. Gao, H. Guo, S. Ha, D. Joseph-McCarthy, L. Kuchnir, K. Kuczera, F. T. K. Lau, C. Mattos, S. Michnick, T. Ngo, D. T. Nguyen, B. Prodhom, W. E. Reiher III, B. Roux, M. Schlenkrich, J. C. Smith, R. Stote, J. Straub, M. Watanabe, J. Wiorkiewicz-Kuczera, D. Yin, M. Karplus, *J. Phys. Chem. B* **1998**, *102*, 3586–3616.
- [15] W. L. Jorgensen, J. Chandrasekhar, J. D. Madura, R. W. Impey, M. L. Klein, *J. Chem. Phys.* **1983**, *79*, 926–935.
- [16] J. P. Ryckaert, G. Ciccotti, H. J. C. Berendsen, *J. Comput. Phys.* **1977**, *23*, 327–341.
- [17] a) D. A. Case, T. A. Darden, T. E. Cheatham III, C. L. Simmerling, J. Wang, R. E. Duke, R. Luo, K. M. Merz, B. Wang, D. A. Pearlman, M. Crowley, S. Brozell, V. Tsui, H. Gohlke, J. Mongan, V. Hornak, G. Cui, P. Beroza, C. Schafmeister, J. W. Caldwell, W. S. Ross, P. A. Kollman, *AMBER8*, University of California, San Francisco, **2004**; b) D. A. Case, T. E. Cheatham, T. Darden, H. Gohlke, R. Luo, K. M. Merz Jr., A. Onufriev, C. Simmerling, B. Wang, R. Woods, *J. Comput. Chem.* **2005**, *26*, 1668–1688.
- [18] Y. Duan, C. Wu, S. Chowdhury, M. C. Lee, G. Xiong, W. Zhang, R. Yang, P. Cieplak, R. Luo, T. Lee, *J. Comput. Chem.* **2003**, *24*, 1999–2012.
- [19] S. Cansu, P. Doruker, *Biochemistry* **2008**, *47*, 1358–1368.
- [20] S. P. Lloyd, *IEEE Trans. Inf. Theory* **1982**, *28*, 129–137.
- [21] M. Feig, J. Karanicolas III, C. L. Brooks, in *MMTSB NIH Research Resource*, The Scripps Research Institute, **2001**.
- [22] G. Gerstein, *Acta Crystallogr.* **1992**, *A48*, 271–276.
- [23] Chemical Computing Group, Montreal, Canada, **2010**.
- [24] X.-G. Gao, E. Maldonado, R. Perez-Montfort, G. Garza-Ramos, M. T. Gomez-Puyou, A. Gomez-Puyou, A. Rodriguez-Romero, *Proc. Natl. Acad. Sci. USA* **1999**, *96*, 10062–10067.
- [25] a) N. Thanki, J. P. Zeelen, M. Mathieu, R. Jaenicke, R. A. Abagyan, R. K. Wierenga, W. Schliebs, *Protein Eng.* **1997**, *10*, 159–167; b) T. V. Borchert, R. Abagyan, R. Jaenicke, R. K. Wierenga, *Proc. Natl. Acad. Sci. USA* **1994**, *91*, 1515–1518.
- [26] S. F. Sousa, P. A. Fernandes, M. J. Ramos, *Proteins: Struct., Funct., Bioinf.* **2006**, *65*, 15–26.

Received: July 27, 2011

Accepted: October 12, 2011

Published online: November 30, 2011